

# Resolution and Super-Resolution in Inverse Diffraction

*M. Bertero, P. Boccacci and M. Piana*

*INFN and Dipartimento di Fisica  
Università di Genova  
Via Dodecaneso 33, 16146 Genova, Italy  
e-mail: bertero@ge.infn.it*

**Abstract.** In this tutorial paper we discuss the concept of resolution in problems of inverse diffraction. These problems have direct applications in areas such as acoustic holography and can also be considered as intermediate steps of more general problems of inverse scattering. We justify the generally accepted principle that the resolution achievable is of the order of the wavelength of the radiation used in the experiment. Moreover we indicate two cases where super-resolution, i.e. resolution beyond the limit of the wavelength, can be achieved. The first is the case of near-field data where super-resolution is possible thanks to the information conveyed by evanescent waves. The second is the case of subwavelength sources, where super-resolution is possible thanks to out-of-band extrapolation of far-field data. Simple algorithms for obtaining this result are also described.

## 1 Introduction

In problems of wave propagation such as those occurring in optics, acoustics, electromagnetism etc., a generally accepted principle is that the resolution achievable about the sources from observations of the scattered or emitted radiation is of the order of the wavelength  $\lambda$  of the radiation. In other words this means that it is only possible to recover details of the source whose linear dimensions are of the order of  $\lambda$ . Moreover one says that in a particular problem super-resolution is achieved if it is possible to obtain a resolution limit much smaller than  $\lambda$ . In this tutorial paper we discuss two problems of inverse diffraction and we use these problems for investigating two cases where super-resolution is achievable.

Inverse diffraction can be defined as the problem of determining the field distribution on a boundary surface  $\Sigma_1$ , from the knowledge of the field distribution on a surface  $\Sigma_2$  situated within the domain where the wave propagates. Such a problem is, implicitly or explicitly, an intermediate step in a problem of inverse scattering: the recovery of the structure of the source (or obstacle)

from observations of the field on a surface  $\Sigma_2$  implies the recovery of the field on a surface  $\Sigma_1$  surrounding the source. Then the resolution in the recovery of the source is roughly of the order of the resolution in the recovery of the field on  $\Sigma_1$ .

We will consider two very simple cases: in the first  $\Sigma_1$  and  $\Sigma_2$  are two parallel planes while in the second  $\Sigma_1$  and  $\Sigma_2$  are two concentric spheres. The first case is of interest both in far field acoustic holography (FAH) (Sondhi 1969) and in near field acoustic holography (NAH) (Williams and Maynard 1980) as well as in the application of holographic techniques to inverse scattering in optics (Wolf 1970), since in these applications the amplitudes are detected over planar surfaces. The second case clearly applies to experiments where the field is observed over a sphere surrounding the sources or scatterers.

In the first case it is possible to define in a precise way the so-called Rayleigh resolution limit which is proportional to  $\lambda$  and which corresponds to the case of far-field data. Then super-resolution is possible or by the use of *a priori* information about the source if only far-field data are available or by the use of near-field data by taking advantage of the information conveyed by evanescent waves.

In the case of spherical surfaces one can also consider the two problems, that with far-field data and that with near-field data. For the first problem the data are the values of the so-called diffraction pattern, which coincides with the scattering amplitude in the case of a scattering experiment. For the second problem the data are the values of the field amplitude over a sphere surrounding the sources. For the inverse diffraction problems corresponding to these situations it is possible to show, by investigating the behaviour of the eigenvalues of the propagation operators, that effects similar to those occurring for planar surfaces must also hold true, even if the analysis is essentially qualitative.

Finally, in the last section, we describe methods which can be used for the restoration of objects of the order of the wavelength from far-field data. We also briefly discuss the effect of different constraints on the regularized solution in these circumstances.

## 2 Inverse diffraction from plane to plane

Let the sources of a monochromatic field,  $u(\mathbf{r}) = u(x_1, x_2, x_3)$ , be located in the half-space  $x_3 < 0$ : we consider the free propagation in the half-space  $x_3 > 0$ . Then in this region the field amplitude  $u$  is a solution of the Helmholtz equation

$$\Delta u + k^2 u = 0 \quad , \quad x_3 > 0 \quad (2.1)$$

where  $k$  is the wavenumber, related to the wavelength  $\lambda$  by

$$k = \frac{2\pi}{\lambda} \quad . \quad (2.2)$$

There exists a unique solution of equation (2.1) satisfying the following conditions:

1. Sommerfeld radiation condition at infinity

$$\lim_{r \rightarrow \infty} r \left( \frac{\partial u}{\partial r} - iku \right) = 0 \quad , \quad r = \sqrt{x_1^2 + x_2^2 + x_3^2} \quad ; \quad (2.3)$$

2. a boundary condition on the plane  $x_3 = 0$  (the source plane)

$$u(x_1, x_2, 0) = f(x_1, x_2) \quad . \quad (2.4)$$

In general it is reasonable to assume that  $f$  is a square-integrable function.

It has been proved by Sommerfeld (Sommerfeld 1896) that there exists a unique solution of this problem, which is given by

$$u(x_1, x_2, x_3) = \int_{-\infty}^{+\infty} \int_{-\infty}^{+\infty} G^{(+)}(x_1 - x'_1, x_2 - x'_2, x_3) f(x'_1, x'_2) dx'_1 dx'_2 \quad (2.5)$$

where

$$G^{(+)}(\mathbf{r}) = -\frac{1}{2\pi} \frac{\partial}{\partial x_3} \frac{e^{ikr}}{r} \quad (2.6)$$

is the (forward) Green function of the problem. However, for the discussion of the inverse diffraction problem, the so-called representation in terms of an *angular spectrum of plane waves* (Shewell and Wolf 1968) is more useful.

Let us consider the plane  $x_3 = a > 0$  and let us denote by  $\rho = \{x_1, x_2\}$  the position of a point in a plane orthogonal to the  $x_3$ -axis. Then the amplitude  $u_a(\rho) = u(x_1, x_2, a)$  of the field on the plane  $x_3 = a$  can be written as a convolution product

$$u_a(\rho) = (S_a^{(+)} * f)(\rho) \quad (2.7)$$

where  $S_a^{(+)}(\rho) = G^{(+)}(x_1, x_2, a)$  acts as a *point spread function* (PSF). The Fourier transform of  $S_a^{(+)}$ , i.e. the *transfer function* (TF) of the system, can be computed and it is given by

$$\hat{S}_a^{(+)}(\omega) = e^{iam(\omega)} \quad (2.8)$$

where  $(|\omega| = \sqrt{\omega_1^2 + \omega_2^2})$

$$m(\omega) = \begin{cases} (k^2 - |\omega|^2)^{\frac{1}{2}} & |\omega| \leq k \\ i(|\omega|^2 - k^2)^{\frac{1}{2}} & |\omega| > k \end{cases} \quad . \quad (2.9)$$

Therefore the transfer function has an oscillatory behaviour at low spatial frequencies (more precisely when  $|\omega| \leq k$ ) while it has an exponential decay, as  $\exp(-a|\omega|)$ , at high spatial frequencies, i.e. when  $|\omega| > k$ . The plane waves with spatial frequencies  $|\omega| < k$  are called *homogeneous waves* while the plane waves with  $|\omega| > k$  are called *evanescent waves*. In figure 1 we plot the real and imaginary part of the PSF  $S_a^{(+)}$  as a function of  $\rho = |\rho|$ , for two values

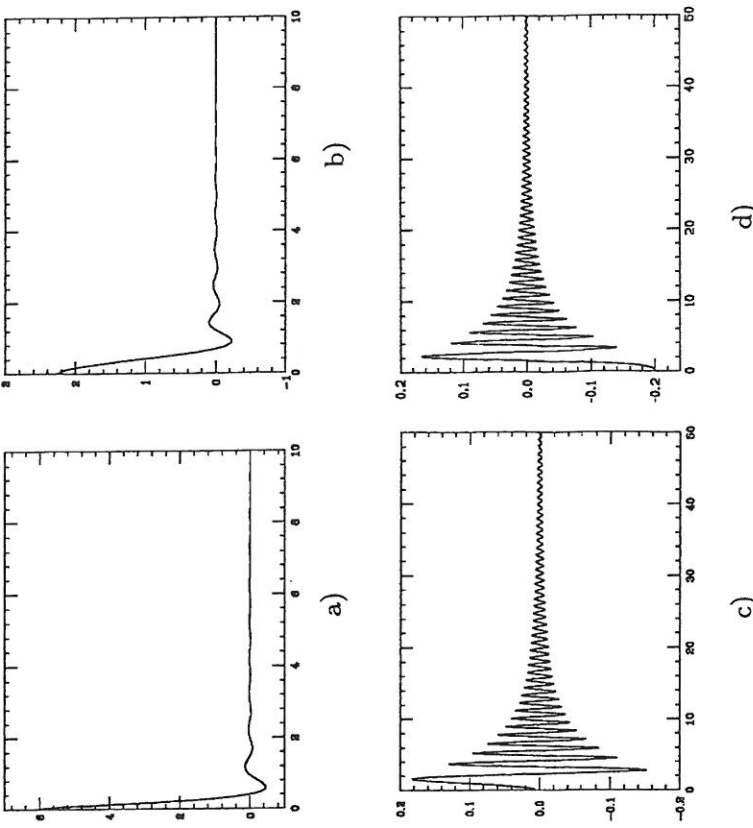


**Fig. 1.** Plot of the real and imaginary part of  $S_a^{(-)}$ , as a function of  $x := \rho/\lambda$ , for  $a = \lambda/5$  (panels a) and b), corresponding to the near-field region and for  $a = 5\lambda$  (panels c) and d)), corresponding to the far-field region.

of  $a = \lambda/5$  and  $a = 5\lambda$ . When  $a < \lambda$  the PSF has a rather narrow central peak and small side-lobes. In fact the PSF tends to a Dirac delta function when  $a \rightarrow 0$ . On the other hand, when  $a > \lambda$ , the PSF shows oscillations with roughly equispaced zeroes, the distance between adjacent zeroes being of the order of  $\lambda/2$ . These different behaviours correspond to different behaviours of the transfer function  $\hat{S}_a^{(+)}$ . In figure 2 we plot the modulus of  $\hat{S}_a^{(+)}$  as a function of  $\omega = |\omega|$ , for the same values of  $a$  used in figure 1. The modulus of the transfer function is one up to  $\lambda\omega = 2\pi$  and then decays exponentially for  $\lambda\omega > 2\pi$ . In the case  $a = 5\lambda$  it is so sharp that the modulus of the transfer function is very close to a step function.

The previous analysis clearly indicates that the effect of propagation can be described in terms of a Fourier filter, more precisely a low pass Fourier filter and that two distinct spatial regions can be considered:

- *Near-field region*: corresponds to distances  $a < \lambda$ ; in such a case the contribution of evanescent waves is important.
- *Far-field region*: corresponds to distances  $a > \lambda$ ; in such a case the contribution of evanescent waves is negligible; one can assume that the field amplitude  $u_a(\rho)$  is band-limited with a band given by

$$\mathcal{B} = \{\omega, |\omega| \leq k\} \quad (2.10)$$

We can formulate now the problem of *inverse diffraction from plane to plane: evaluate the field amplitude  $f(\rho)$  on the boundary plane  $x_3 = 0$ , being given the field amplitude  $g(\rho) = u_a(\rho)$  (corrupted by noise or experimental errors) on the plane  $x_3 = a$ .*

## 2.1 Inverse diffraction from far-field data

In this case evanescent waves can be completely neglected. Therefore the inverse diffraction problem is equivalent to solve a convolution equation where the PSF  $S_a^{(+)}$  is a band-limited function with band  $\mathcal{B}$ , equation (2.10), i.e.  $\hat{S}_a^{(+)}(\omega) = \exp[iam(\omega)]$  when  $|\omega| < k$  and  $\hat{S}_a^{(+)}(\omega) = 0$  when  $|\omega| > k$ . Its inverse Fourier transform  $S_a^{(+)}(\rho)$  will be called the *forward propagation kernel*.

It is obvious that the solution of the problem  $g = S_a^{(+)} * f$  is not unique; moreover it may not exist if  $g$  is affected by out-of-band noise. However, in such a case, the ill-posedness of the problem is not very serious and it can be cured by considering the *generalized solution*, i.e. the least-squares solution of minimal norm (Groetsch 1977).

It is very easy to prove that the generalized solution  $f^\dagger(\rho)$  can be written as follows

$$f^\dagger(\rho) = (S_a^{(-)} * g)(\rho) \quad (2.11)$$

$$g = S_a^{(+)} * f + w \quad (2.13)$$

$$f^\dagger = (S_a^{(-)} * S_a^{(+)} * f + S_a^{(-)} * w) \quad (2.14)$$

The problem of determining the generalized solution is well-posed. If we assume that the data are given by

where  $w$  is a term describing noise or experimental errors, then from equation (2.11) and (2.13) we obtain

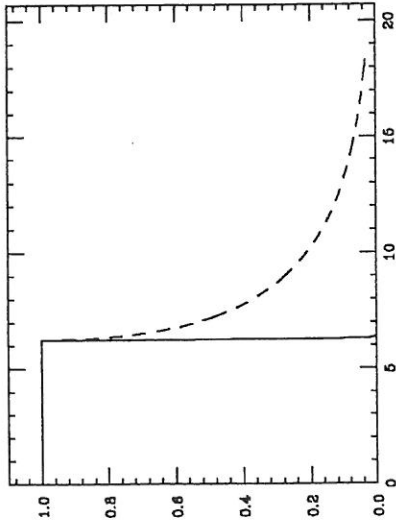


Fig. 2. Plot of the modulus of the TF  $S_a^+(\omega)$ , as a function of  $\xi = \lambda\omega$ , for the values of  $a$  of figure 1:  $a = \lambda/5$  (dashed line) and  $a = 5\lambda$  (solid line).

The term  $S_a^{(-)} * w$  is the noise contribution to the generalized solution. Its  $L^2$ -norm is smaller than the  $L^2$ -norm of the noise: since the out-of-band noise does not contribute to  $S_a^{(-)} * w$ , from equation (2.12) and Parseval equality one easily derives that  $\|S_a^{(-)} * w\| \leq \|w\|$ . As concerns the first term, the kernel  $H_B = S_a^{(-)} * S_a^{(+)}$  is the inverse Fourier transform of the characteristic function of the band  $B$ , equation (2.10), and therefore it is given by

$$H_B(\rho) = \frac{1}{(2\pi)^2} \int_B e^{i\rho \cdot \omega} d\omega = \frac{k}{2\pi} \frac{J_1(k|\rho|)}{|\rho|}. \quad (2.15)$$

We conclude that:

1. The generalized solution  $f^\dagger$  is a noisy band-limited approximation of the boundary amplitude  $f$ .
2. The kernel  $H_B(\rho)$  has a central peak at  $\rho = 0$  and is zero over circles with centre the origin and radii proportional to the zeros of the Bessel function  $J_1(t)$ .

The radius of the first circle is given by

$$R = 1.22 \frac{\pi}{k} = 1.22 \frac{\lambda}{2} \quad (2.16)$$

and this is the famous *Rayleigh resolution limit* (Born and Wolf 1980). It is the radius of the central peak of the function  $H_B(\rho)$  and it provides a measure of the smallest details of  $f(\rho)$  which are recoverable. Moreover it is closely connected to the size of the band  $B$ : the larger is the radius of the band, the smaller is the resolution distance.

In figure 3 we give two examples of restorations of binary objects obtained by means of the generalized solution  $f^\dagger$ . They make evident that details of the order of the wavelength are recovered, while details smaller than the wavelength are not. In fact the first object is a grid which does not contain details smaller than the wavelength, while the second one contains details of the order of  $\lambda/2$ . The images of the two objects are computed on the plane  $a = 5\lambda$  and are contaminated by white gaussian noise (with  $\sigma = 0.01$ , about 1% of the maximum value of the field amplitude). The restoration of the first object, provided by equation (2.11), clearly shows the vertical and horizontal bars, which are  $1\lambda$  wide. In the restoration of the second object the bars are essentially lost, in agreement with the Rayleigh criterion.

Now, the Rayleigh limit (2.16) is related to the radius  $k$  of the band of the generalized solution (2.11), more precisely it is proportional to the inverse of this radius. Therefore, in order to obtain a resolution better than the Rayleigh limit, it should be necessary to increase the band, i.e. to extrapolate the generalized solution outside  $B$ . This is possible, in principle, if the Fourier transform of the unknown amplitude  $f$  is analytic and a sufficient condition for the analyticity of  $f$  is the boundedness of the support of  $f$ .

In order to investigate the consequences of this condition, one can proceed as follows. First recover (noisy) values of  $\hat{f}(\omega)$  inside  $B$  by computing the generalized solution  $f^\dagger(\rho)$ . If we neglect the noise term, from equations (2.14) and (2.15) we obtain that

$$f^\dagger = H_B * f. \quad (2.17)$$

This convolution operator is the band-limiting operator which projects  $f$  onto the subspace of the functions whose band is interior to the band  $B$ , equation (2.10). Next, if we have *a priori* information about the support of  $f$  and, in particular, if we know that its support is interior to some bounded domain  $D$  of the plane, then we can restrict the convolution operator (2.17) to the subspace of functions whose support is interior to  $D$ . This is equivalent to introduce the following operator from  $L^2(D)$  into  $L^2(R^2)$

$$(Af)(\rho) = \int_D H_B(\rho - \rho') f(\rho') d\rho'. \quad (2.18)$$

Then extrapolation of  $\hat{f}$  outside  $B$  is equivalent to solve the equation

$$f^\dagger = Af. \quad (2.19)$$

In fact, in the absence of noise, this equation has a unique solution whose support is interior to  $D$  and whose Fourier transform coincides with  $\hat{f}(\omega)$  over  $B$ .

However the problem (2.19) is ill-posed. The operator  $A : L^2(D) \rightarrow L^2(R^2)$  is a compact and injective operator. Its singular functions are related to the *generalized prolate spheroidal functions* introduced by Slepian (1964) and its singular values are the square roots of the eigenvalues associated with these functions. By investigating the singular value spectrum of the operator (2.18) and by using the most simple regularization techniques

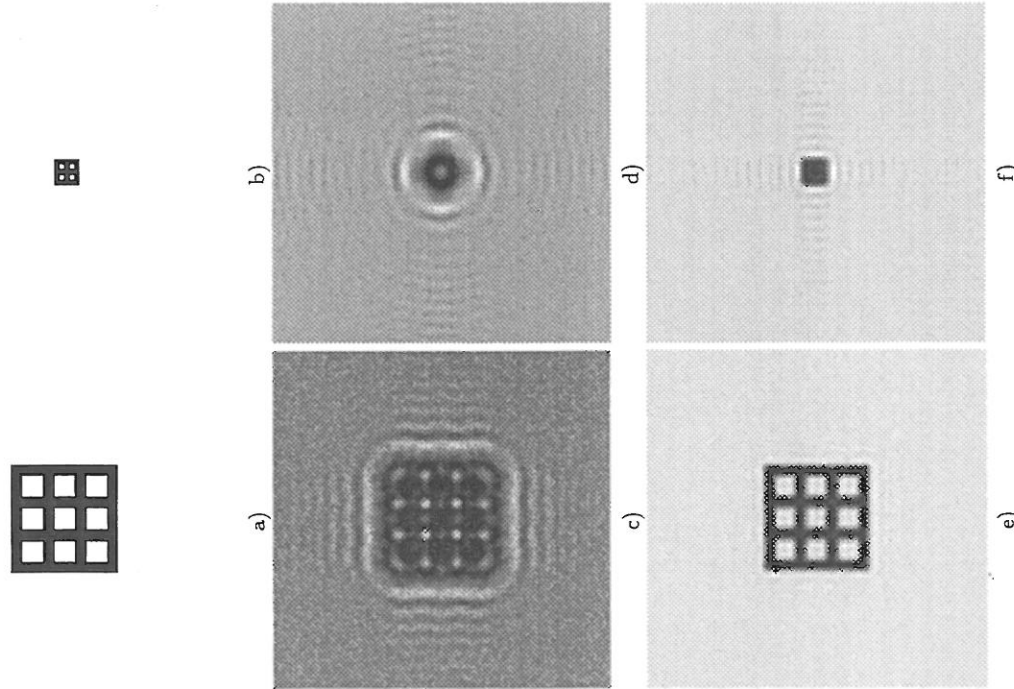


**Fig. 3.** Two examples of restorations obtained by means of the generalized solution (2.11). Panel a) is a grid  $10\lambda$  wide with vertical and horizontal bars  $1\lambda$  wide; panel b) is a grid  $2.5\lambda$  wide with bars  $0.5\lambda$  wide. Panels c) and d) show the modulus of the corresponding images on the plane  $\sigma = 5\lambda$ . Panels e) and f) show the restorations provided by the generalized solution (2.11).

(truncated singular functions expansion) it is possible to obtain the following result (Bertero and Pike 1982): if  $\mathcal{D}$  is a disc of radius  $d$ , then it is possible to obtain a significant out-of-band extrapolation (and therefore a significant improvement of resolution) for reasonable values of the signal-to-noise ratio, if the quantity  $c = kd$  is not much larger than one. In other words, super-resolution is feasible when the size of the region where  $f$  is different from zero is of the order of the wavelength  $\lambda$ . We observe that the second object of figure 3 satisfies this condition. Such objects are sometimes referred to as *subwavelength sources*.

In general, the computation of the singular system of the operator (2.18) is difficult and therefore singular function expansions cannot be used for improving Rayleigh resolution limit in 2-D problems. However a very simple iterative method, only based on Fourier transform, was proposed by Gerchberg (Gerchberg 1974). Since it can be proved that this method is equivalent to the well-known Landweber method (De Santis and Gori 1975), it follows that it is equivalent to a filtering of the singular function expansion of the solution, which can be obtained without computing the singular system of the operator. A more general algorithm for super-resolution will be discussed in section 4.

## 2.2 Inverse diffraction from near-field data

As we already remarked the near-field region corresponds to distances between the two planes smaller than the wavelength  $\lambda$ . This condition is satisfied, for instance, in *near-field acoustic holography* (NAH) (Williams and Maynard 1980) and in *scanning near-field optical microscopy* (SNOM) (Pohl and Courijon 1993).

In such a case the information conveyed by evanescent waves allows to increase the resolution beyond the Rayleigh limit. If we consider again the integral equation  $g = S_a^{(+)} * f$ , where  $S_a^{(+)}$  is given now by equations (2.8) - (2.9), the solution of this equation is unique but the problem is still ill-posed as a consequence of the exponential decay of  $S_a^{(+)}(\omega)$  when  $|\omega| > k$ . The most simple regularized solution of the problem can be obtained by a truncated Fourier transform inversion. If we have an estimate  $\epsilon$  of the norm of the noise and an estimate  $E$  of the norm of the boundary amplitude  $f$ , then an estimate  $\tilde{f}$  of  $f$  satisfying the bound  $E$  and reproducing the data within an error  $\epsilon$  is given by

$$\tilde{f}(\omega) = \begin{cases} e^{-i\omega m(\omega)} \hat{g}(\omega) & |\omega| < k_{\text{eff}} \\ 0 & |\omega| > k_{\text{eff}} \end{cases} \quad (2.20)$$

$$k_{\text{eff}} = \max\{|\omega|, |\hat{S}_a^{(+)}(\omega)| \geq \frac{\epsilon}{E}\} \quad (2.21)$$

This is a particular case of the methods, based on truncated spectral representations, investigated by Miller (Miller 1970).

Since  $\epsilon/E < 1$ , the condition in equation (2.21) can be replaced by the following one

$$\exp[a(|\omega|^2 - k^2)^{\frac{1}{2}}] \leq \frac{\epsilon}{E} \quad (2.22)$$

and one easily finds that

$$k_{\text{eff}} = k \left[ 1 + \frac{1}{(ka)^2} \log^2 \left( \frac{E}{\epsilon} \right) \right] . \quad (2.23)$$

The regularized solution  $\tilde{f}$  is still bandlimited with a band  $B_{\text{eff}}$  which is a disc of radius  $k_{\text{eff}}$ :

$$\tilde{f}(\rho) = \frac{1}{(2\pi)^2} \int_{B_{\text{eff}}} e^{-iam(\omega)} \hat{g}(\omega) e^{i\rho\omega} d\omega . \quad (2.24)$$

By applying the Rayleigh criterion one finds that the resolution limit is now given by

$$R_{\text{eff}} = 1.22 \frac{\pi}{k_{\text{eff}}} \simeq \left( \frac{ka}{\log(\frac{E}{\epsilon})} \right)^2 R , \quad (2.25)$$

where the factor 1 in the r.h.s. of equation (2.23) has been neglected.

We point out that this resolution distance depends on the distance between the two planes and, in fact, it decreases quadratically when  $a$  decreases. Moreover it depends logarithmically on the signal-to-noise ratio  $\frac{E}{\epsilon}$  and it decreases when  $\frac{E}{\epsilon}$  increases.

In order to give an idea of the considerable improvement of resolution which can be achieved in this way, we consider the case of acoustic waves with a frequency of 3.3 kHz (we remind that the range of frequencies of acoustic waves is between 20 Hz and 20 kHz). The corresponding wavelength is about 10 cm and therefore the Rayleigh resolution distance (2.16) is about 6 cm. Now, if we assume to collect data at the distance of 1 cm from the source plane and if we also assume that the signal-to-noise ratio  $E/\epsilon$  is of the order of 100, then from equations (2.23) and (2.25) we derive that  $R_{\text{eff}} \simeq 0.11$  cm, with an improvement, with respect to the Rayleigh limit, by a factor 54. If we should be able to collect data at a distance of 1 mm, then we should have an improvement by a factor 5400. If  $E/\epsilon = 10$  then these figures must be reduced by a factor 4 but they still imply a spectacular improvement of resolution.

### 3 Inverse diffraction from sphere to sphere

In the previous section we investigated the case of planar surfaces and we considered two cases of super-resolution: a) sources of the order of the wavelength in the case of far-field data; b) sources of arbitrary size in the case of near-field data. The most significant improvement of resolution can be obtained in the second case.

It is expected that similar results apply also to other surfaces, in particular closed and bounded surfaces. It is interesting to note that, for these surfaces, we have uniqueness of the solution also in the case of far-field data. The problem, however, is still ill-posed because the solution does not exist for arbitrary data and, when it exists, does not depend continuously on the data. In order to clarify these points we investigate the case of spherical surfaces.

Assume that  $\Sigma_1$  is a sphere, with centre the origin and radius  $a_1$ , containing all the sources (or scatterers) of the radiation field. Then the solution of the diffraction problem consists in determining a solution  $u = u(r, \theta, \phi)$  of the Helmholtz equation (2.1) in the region  $r > a_1$  satisfying Sommerfeld radiation condition (2.3) at infinity and also a boundary condition on the sphere  $r = a_1$

$$u(a_1, \theta, \phi) = f(\theta, \phi) \quad (3.1)$$

where  $f$  is a given function (direct problem). The solution of this diffraction problem can be easily obtained by means of expansions in terms of the spherical harmonics  $Y_{l,m}$ . If we denote by  $f_{l,m}$  the expansion coefficients of the boundary data  $f$

$$f_{l,m} = \int_{\Omega} f(\theta, \phi) Y_{l,m}^*(\theta, \phi) d\Omega , \quad (3.2)$$

where  $\Omega$  is the unit sphere and  $d\Omega = \sin \theta d\theta d\phi$ , then the spherical harmonics expansion of  $u(r, \theta, \phi)$  is given by

$$u(r, \theta, \phi) = \sum_{l,m} f_{l,m} \frac{h_l^{(1)}(kr)}{h_l^{(1)}(ka_1)} Y_{l,m}(\theta, \phi) \quad (3.3)$$

where the functions  $h_l^{(1)}(r) = (\pi/2r)^{\frac{1}{2}} H_{l+\frac{1}{2}}^{(1)}(r)$  are the spherical Hankel functions of the first kind.

The inverse diffraction problem can now be formulated as follows: given the values of the field amplitude on the sphere  $\Sigma_2$  with centre the origin and radius  $a_2 > a_1$ , determine the unknown field amplitude  $f$  on the boundary sphere  $a_1$ . This problem is, in fact, equivalent to the inversion of the following integral operator  $A : L^2(\Omega) \rightarrow L^2(\Omega)$

$$(Af)(\theta, \phi) = \int_{\Omega} S^{(+)}(\theta, \phi; \theta', \phi') f(\theta', \phi') d\Omega' \quad (3.4)$$

where

$$S^{(+)}(\theta, \phi; \theta', \phi') = \sum_{l,m} \frac{h_l^{(1)}(ka_2)}{h_l^{(1)}(ka_1)} Y_{l,m}(\theta, \phi) Y_{l,m}(\theta', \phi') . \quad (3.5)$$

This is a compact operator and its eigenvalues  $\lambda_l$ , with multiplicity  $2l+1$ , are given by

$$\lambda_l = \frac{h_l^{(1)}(ka_2)}{h_l^{(1)}(ka_1)} . \quad (3.6)$$

Since for large  $l$  one has

$$\lambda_l \simeq \exp[-(l+1) \log(\frac{a_2}{a_1})] , \quad (3.7)$$

the problem is severely ill-posed. However the exponential decay of the eigenvalues decreases when the ratio  $a_2/a_1$  decreases. It follows that, if we regularize the problem by considering truncated spherical harmonics expansions, one can recover more and more terms as the sphere  $\Sigma_2$  approaches the sphere  $\Sigma_1$ . This is an effect which is due again to evanescent waves even if a clear distinction between evanescent and homogeneous waves does not appear from the expansion (3.3). In fact, to this purpose, a much deeper analysis of the solutions of the wave equation is needed (Levi and Keller 1959).

As concerns the problem with far-field data, one can now consider the asymptotic case  $r \rightarrow \infty$ . From the asymptotic behaviour of the spherical Hankel functions

$$h_l^{(1)}(r) \simeq (-i)^{l+1} \frac{e^{ikr}}{r} \quad (3.8)$$

one obtains the asymptotic behaviour of the field amplitude (3.3)

$$u(r, \theta, \phi) \simeq \frac{e^{ikr}}{r} g(\theta, \phi) \quad (3.9)$$

where

$$g(\theta, \phi) = \sum_{l,m} (-i)^{l+1} \frac{f_{l,m}}{h_l^{(1)}(ka_1)} Y_{l,m}(\theta, \phi) . \quad (3.10)$$

The function  $g(\theta, \phi)$  is usually called *diffraction pattern* and is related to the scattering amplitude in the case of scattering problems. The problem of inverse diffraction from far-field data can now be formulated as the problem of estimating the boundary function  $f(\theta, \phi)$  from knowledge of the diffraction pattern  $g(\theta, \phi)$ . This problem, which is still ill-posed and, in fact, much more ill-posed than the problem of inverse diffraction from near-field data, can be formulated as the inversion of the integral operator

$$(Af)(\theta, \phi) = \int_{\Omega} S_{\infty}^{(+)}(\theta, \phi; \theta', \phi') f(\theta', \phi') d\Omega' \quad (3.11)$$

where

$$S_{\infty}^{(+)}(\theta, \phi; \theta', \phi') = \sum_{l,m} \frac{(-i)^{l+1}}{h_l^{(1)}(ka_1)} Y_{l,m}(\theta, \phi) Y_{l,m}^*(\theta', \phi') . \quad (3.12)$$

This is a compact operator in  $L^2(\Omega)$  and it is also injective (uniqueness of the solution of the inverse diffraction problem with far-field data). Its eigenvalues are given by

$$\lambda_l = \frac{(-i)^{l+1}}{h_l^{(1)}(ka_1)} \quad (3.13)$$

and they tend to zero much more rapidly than the eigenvalues (3.6) of the problem with near-field data. In fact their asymptotic behaviour is  $|\lambda_l| \simeq \exp[-l \log(2l/ek a_1)]$ .

An analysis of super-resolution in the case of far-field data has not yet been performed. It is reasonable to conjecture that super-resolution can be obtained in the case where the radius  $a_1$  of the sphere is of the order of the wavelength of the radiation. An indication in this direction has been obtained by an analysis of the inverse scattering problem in the case of Born approximation (Habashy and Wolf 1994).

#### 4 An algorithm for super-resolution

We come back now to the problem of inverse diffraction from plane to plane, section 2, and we describe an algorithm which can be used for achieving super-resolution when *a priori* information about the support of the boundary function  $f(\rho)$  is available.

At the end of section 2.1 we mentioned the Gerchberg algorithm which can be used for this purpose. However this algorithm cannot be applied directly to a convolution problem such as that described by equation (2.7). One must first estimate the Fourier transform of  $f(\rho)$  over an effective band (for instance the disc of radius  $k$ , as in section 2.1, or the disc of radius  $k_{\text{eff}}$ , as in section 2.2); then one can use Gerchberg algorithm for extrapolating the Fourier transform of  $f(\rho)$  outside the effective band.

We describe now an algorithm which is a generalization of the Gerchberg algorithm and does not require to solve the problem in two steps. For generality, we consider a bounded convolution operator

$$(Af)(\rho) = (K * f)(\rho) \quad (4.1)$$

and the associated first kind equation

$$Af = g \quad (4.2)$$

where  $g$  is a given function, the data of the problem. We also assume that  $f$  belongs to the subspace of functions whose support is inferior to a given and bounded domain  $\mathcal{D}$ . The projection operator onto this subspace is given by

$$(P_{\mathcal{D}} f)(\rho) = \chi_{\mathcal{D}}(\rho) f(\rho) \quad (4.3)$$

where  $\chi_{\mathcal{D}}(\rho)$  is the characteristic function of the domain  $\mathcal{D}$ .

Under rather broad conditions on the PSF  $K(\rho)$ , the operator  $AP_{\mathcal{D}}$  is compact and regularized solutions of the equation

$$AP_{\mathcal{D}} f = g \quad (4.4)$$

are provided by the *Landweber method*

$$f_{n+1} = f_n + \tau P_{\mathcal{D}}(A^* g - A^* AP_{\mathcal{D}} f_n) \quad (4.5)$$

where  $\tau$  is the relaxation parameter, satisfying the usual conditions

$$0 < \tau < \frac{2}{\|A\|^2} \quad (4.6)$$

In the case  $f_0 = 0$ , it is easy to show by induction that all the iterates  $f_n$  satisfy the condition  $P_D f_n = f_n$ . Therefore the method (4.5) is equivalent to the following projected Landweber method

$$f_{n+1} = P_D f_n + \tau P_D (A^* g - A^* A f_n) \quad (4.7)$$

From this equation one can easily derive that the algorithm can be implemented using only the Fourier transform. In fact, if  $f_n(\rho)$  has been computed, then one can compute  $\hat{f}_n(\omega)$  and by  $\hat{f}_n(\omega)$  the function

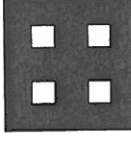
$$\hat{h}_{n+1}(\omega) = \hat{f}_n(\omega) + \tau (\hat{K}^*(\omega) \hat{g}(\omega) - |\hat{K}(\omega)|^2 \hat{f}_n(\omega)) \quad (4.8)$$

The last step consists in computing the inverse Fourier transform of  $\hat{h}_{n+1}(\omega)$ ,  $h_{n+1}(\rho)$ , and in projecting this function by means of  $P_D$  in order to obtain  $f_{n+1}(\rho) = (P_D h_{n+1})(\rho)$ .

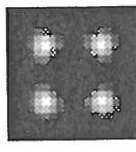
The advantage of this method is that it does not require the use of the singular functions of the operator  $AP_D$  and therefore can be easily implemented.

In figure 4 we give an example of restoration obtained by means of this method. The object in figure 4(a) is the smaller object of figure 3, i.e. a grid with size  $2.5\lambda$ , therefore of the order of  $\lambda$  as required for achieving super-resolution from far-field data. The data are the same of figure 3(d), i.e. the noisy amplitude on the plane with  $a = 5\lambda$ . The restoration of this object provided by algorithm (4.7) is represented in figure 4(b) where it is evident the recovery of the four square holes, with size  $0.5\lambda$  each, which are completely lost in the generalized solution of figure 3(f). The support used is just the square with size  $2.5\lambda$ . If we do not have this information, it can be inferred from the data by performing inversions with different supports. We note that the super-resolution effect is just the one described at the end of section 2.1.

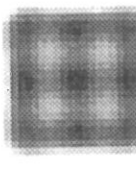
In (Piana and Bertero 1996) it has been pointed out that the iteration (4.7) defines a regularization algorithm. In fact, if the data  $g$  is not affected by noise and if  $f_0 = 0$  the sequence  $\{f_n\}_{n=1}^\infty$  defined by equation (4.7) converges to the unique solution of equation (4.4) in the strong topology of  $L^2$ . Moreover, in presence of noise, the algorithm is characterized by the so-called semiconvergence property, i.e. the restoration error  $\|f_n - f\|$  decreases first and increases later with respect to the number of iterations. This means that in this method the number of iterations plays the role of the regularization parameter. In order to determine the optimum value of this number, several "ad hoc" criterions have been formulated in the case of real data. Things are significantly simpler when the data function is obtained synthetically, since, in this case, the theoretical model  $f$  is explicitly known and the best number of iterations can be obtained by minimizing  $\|f - f_n\|$  with respect to  $n$ .



a)



b)



c)

**Fig. 4.** Example of restoration obtained by means of the projected Landweber method. Panel a) is the smaller grid in figure 3. Panels b) and c) show the restorations provided by the method, by using respectively the constraint of compact support and the constraint of upper bound. Finally panel d) shows the effect of the combined use of the compact support and the positivity constraints.

When, as in the present example, the behaviour of this restoration error is characterized by an extremely flat minimum, it is possible to stop the iteration before the minimum is reached, without a significant loss of accuracy in the restoration. In the case of figure 4(b) it is  $n = 100$ .

However, in general, a notable acceleration of the projected Landweber method can be obtained by means of the so-called *preconditioning*. This procedure consists in the application of the algorithm to a modified least-squares problem. In several numerical examples regarding one dimensional models, it has been shown (Piana and Bertero 1996) that the application of preconditioning allows to obtain a gain in convergence speed up to a factor ten with no substantial modifications in the reconstructions.

The projected Landweber method can be readily generalized to the restoration of functions which belong to a closed convex subset  $C$  of the source space. In this case, the convex non-linear projection operator  $P_C$  can be introduced and the constrained algorithm becomes

$$f_{n+1} = P_C(f_n + \tau A^* g - \tau A^* A f_n) \quad (4.9)$$

The method is now non-linear and the convergence of the iteration (4.9) to the generalized solution has been shown only in the weak topology. Nevertheless, numerical evidence of the strong convergence is provided by several examples.

The algorithm (4.9) can be used when it is necessary to impose upper or lower bounds on the solution. A typical lower bound is provided, for instance, by positivity. These constraints are, in general, useful in order to reduce the ringing effects which appear when linear methods are used for restoring discontinuous objects. For these constraints  $P_C$  is easily computable as well as in the case where one wishes to combine the support constraint with upper or lower bound constraints.

The object of figure 4(a) is a binary object which takes only the values 0 and 1. Therefore these values can be used as lower and upper bounds. In figure 4(c) we give the restoration obtained by means of the algorithm (4.9) after 100 iterations when only the upper bound is imposed. It is remarkable that a super-resolution effect is obtained without using the constraint on the support. This is probably due to the reduction of the ringing effects which are evident in the generalized solution (see figure 3(f)). In this example, the constraint of positivity is useless because the generalized solution of figure 3(f) does not take negative values. This is not true for the restoration of figure 4(b). Therefore in such a case positivity can be useful. In figure 4(d) we give the result obtained by combining positivity and support constraint. It is evident that the restoration is quite good.

Miller K. (1970): Least squares method for ill-posed problems with a prescribed bound *SIAM J. Math. Anal.* 1 52-74.

Piana M. and Bertero M. (1996): Projected Landweber method and preconditioning *Inverse Problems* (in press).

Pohl D. W. and Courjon D. eds. (1993): *Near-Field Optics* (Kluwer, Dordrecht).

Shewell J. R. and Wolf E. (1968): Inverse diffraction and a new reciprocity theorem *J. Opt. Soc. Am.* 58 1596-1603.

Slepian D. (1964): Prolate spheroidal wave functions, Fourier analysis and uncertainty - IV: Extensions to many dimensions, generalized prolate spheroidal functions *Bell Syst. Syst. Tech. J.* 43 3009-3057.

Sommerfeld A. (1896): Mathematische theorie der diffraction *Math. Ann.* 47 317-336.

Sondhi M. M. (1969): Reconstruction of objects from their sound-diffraction patterns *J. Acoust. Soc. Am.* 4b 1158-1164.

Williams E. G. and Maynard J. D. (1980): Holographic imaging without the wavelength resolution limit *Phys. Rev. Lett.* 45 554-557.

Wolf E. (1970): Determination of the amplitude and the phase of scattered fields by holography *J. Opt. Soc. Am.* 60 18-20.

## References

- Bertero M. and Pike E. R. (1982): Resolution in diffraction-limited imaging, a singular value analysis - I: The case of coherent illumination *Opt. Acta* 29 727-746.
- Born M. and Wolf E. (1980): *Principles of Optics* (Pergamon Press, Oxford).
- De Santis P. and Gori F. (1975): On an iterative method for super-resolution *Opt. Acta* 22 691-695.
- Gerchberg R. W. (1974): Super-resolution through error energy reduction *Opt. Acta* 21 709-720.
- Groetsch C. W. (1977): *Generalized Inverses of Linear Operators* (Dekker, New York).
- Habashy T. and Wolf E. (1994): Reconstruction of scattering potentials from incomplete data *J. Modern Opt.* 41 1679-1685.
- Levi B. R. and Keller G. B. (1959): Diffraction by a smooth object *Comm. Pure Appl. Math.* 12 159-209.